The contribution of metabolic and adipose tissue inflammation to non-alcoholic fatty liver disease

Mulder, P.C.A.

Chapter 7

Macrovesicular steatosis is associated with development of lobular inflammation and fibrosis in diet-induced non-alcoholic steatohepatitis (NASH)

Petra Mulder[1,2], Wen Liang[1,3], P.Y. Wielinga[1], Lars Verschuren[4], Karin Toet[1], Louis M. Havekes[1,3], Anita M. van den Hoek[1]*, Robert Kleemann[1, 2, 5]*

[1] The Dutch Organization for Applied Scientific Research (TNO), Department of Metabolic Health Research, Leiden, 2333 CK, The Netherlands
[2] Leiden University Medical Center, Department of Cardiovascular Surgery, Leiden, 2333 ZA, The Netherlands
[3] Leiden University Medical Center, Department of Endocrinology and Cardiology, Leiden, 2333 ZA, The Netherlands
[4] The Dutch Organization for Applied Scientific Research (TNO), Department of Microbiology and Systems Biology, Zeist, 3704 HE, The Netherlands
[5] Wageningen University, Department of Human and Animal Physiology, Wageningen, 6709 PJ, The Netherlands

*These authors contributed equally to the manuscript

Inflammation and Cell Signaling. 2015 Jun 8;2(3).

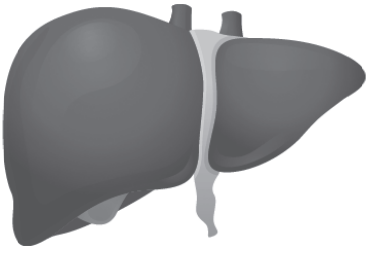

ABSTRACT

Non-alcoholic steatohepatitis (NASH) is characterized by liver steatosis and lobular inflammation. It is unclear how the development of liver steatosis and the formation of inflammatory cell aggregates are related to each other. The present study investigated the longitudinal development of two forms of steatosis, micro- and macrovesicular steatosis, as well as lobular inflammation. ApoE*3Leiden. CETP (E3L.CETP) transgenic mice were fed a high-fat diet containing 1% w/w cholesterol (HFC) for 12 weeks to induce NASH. Livers were harvested in intervals of 4 weeks and analyzed by histological and biochemical techniques, as well as transcriptome and subsequent pathway analysis. Major findings were validated in independent NASH studies using other rodent models, i.e. HFD-treated C57BL/6J and LDLr-/-.Leiden mice. In E3L.CETP mice, microvesicular steatosis was rapidly induced and reached plateau levels after already 4 weeks of HFC treatment, while macrovesicular steatosis developed more gradually and progressed over time. Lobular inflammation increased after 4 weeks with a significant further progression towards the end of the study (12 weeks). Macrovesicular, but not microvesicular, steatosis was positively correlated with the number of inflammatory aggregates. This correlation was confirmed in a milder (C57BL/6J) and a more severe (LDLr-/-.Leiden) NASH model. Furthermore, collagen staining showed onset of perihepatocellular fibrosis in E3L.CETP mice after 12 weeks of HFC treatment and transcriptome analysis substantiated the activation of pro-fibrotic pathways and genes. Notably, macrovesicular steatosis correlated positively with liver fibrosis in LDLr-/-.Leiden mice with pronounced fibrosis. In conclusion, this study shows that macrovesicular steatosis is associated with lobular inflammation and liver fibrosis in rodent models and highlights the importance of this form of steatosis in the pathogenesis of NASH.

INTRODUCTION

Non-alcoholic fatty liver disease (NAFLD) is associated with visceral obesity, dyslipidemia and insulin resistance and has become a global threat with an estimated prevalence of 15% to 30% of the general population [1,2]. NAFLD covers a spectrum of liver disease ranging from lipid accumulation (simple steatosis) to non-alcoholic steatohepatitis (NASH). NASH is characterized by steatosis with lobular inflammation which can further progress to liver fibrosis and cirrhosis [3]. The pathophysiology that leads to NASH is not well understood, in particular the relationship between the development of steatosis and lobular inflammation is unclear.

Morphologically, hepatic steatosis can manifest in two forms of lipid accumulation, i.e. macrovesicular or microvesicular steatosis. In macrovesicular steatosis, hepatocytes contain a large, single vacuole of fat which fills the cytoplasm and displaces the nucleus to the periphery (see [4] and references therein). By contrast, hepatocytes with microvesicular steatosis contain many small lipid droplets in the cytoplasm [4]. Emerging data indicate that excessive lipid accumulation in liver cells causes lipotoxic hepatocellular injury and inflammation [5]. Lobular inflammation in NASH is characterized by the presence of inflammatory aggregates, i.e. cell clusters containing different types of immune cells such as neutrophils, lymphocytes and macrophages [6,7]. This inflammation is associated with activation of pro-fibrotic signaling cascades involving stellate cells and the production of collagen [6,8]. To date, it is unclear whether the development of inflammation is linked to a specific form of steatosis, i.e. macro- or microvesicular steatosis.

To identify a potential relationship between the two forms of steatosis and development of lobular inflammation (and the progression to fibrosis), we investigated in a longitudinal study the development of macro- and microvesicular steatosis and lobular inflammation up to the stage of early fibrosis. For this we used ApoE*3Leiden.CETP (E3L.CETP) transgenic mice which have a humanized lipoprotein metabolism and develop NASH in the context of obesity and dyslipidemia [7,9]. These mice were treated with a NASH-inducing high-fat diet

containing 24% lard fat and 1% cholesterol (HFC) for 12 weeks and compared to low-fat diet controls. Groups of mice were sacrificed in monthly intervals until NASH with early fibrosis had developed. NAFLD pathology was scored blindly using a recently established grading system for rodents which is based on the human NAS system [10]. Histological analyses and biochemical measurements in conjunction with transcriptome analysis revealed a positive association between macrovesicular steatosis and lobular inflammation as well as early fibrosis. These findings were confirmed in independent studies using diet-inducible models of NASH (i.e. C57BL/6J and LDLr-/-.Leiden mice) and the results show that macrovesicular steatosis has a critical role in the pathogenesis of NASH.

MATERIAL AND METHODS

Animal time-course experiment

Experiments were approved by an independent Animal Care and Use Committee and were in compliance with European Community specifications regarding the use of laboratory animals. APOE*3Leiden (E3L) mice were cross-bred with transgenic mice that express human- cholesteryl ester transfer protein (CETP) to obtain heterozygous E3L.CETP mice [9]. Male E3L.CETP mice (n=70, 16-19 weeks of age) were used in the present study. All animals were housed in a temperature-controlled room with 12-hour light-dark cycling and had ad libitum access to food and water. Mice received a low fat diet (LFD; 10 kcal% lard, Research Diets, New Brunswick, NJ, USA) during a 4-week run-in period. Mice were matched for body weight, plasma cholesterol and triglycerides and one group (n=10) was sacrificed to define the condition at the start of the experiment (t=0). Remaining mice were matched into 6 groups. Three groups (n=10/group) were treated with a NASH-inducing high-fat diet (HFD; D12451; 45 kcal% lard, Research Diets, New Brunswick NJ, USA) supplemented with 1% (w/w) cholesterol (HFC) [7]. As reference for transcriptome analysis, three groups (n=10/group) received a HFD control diet. At 4-week intervals, food intake and body weight were determined and EDTA plasma was collected from the tail vein after 5h of fasting. Mice were sacrificed after 4, 8 or 12 weeks of diet feeding by CO_2 asphyxiation. The

medial liver lobe was fixed in formalin and embedded in paraffin for histological analysis of NAFLD and the left lateral liver lobe (lobus sinister hepatis) was snap frozen in liquid nitrogen and stored at -80°C for liver lipids, biochemical and gene expression analyses. White adipose tissue was collected, weighed and stored at -80°C.

Histological evaluation of NAFLD

NASH development was assessed histologically in hematoxylin and eosin (HE)-stained liver sections (3 μM) using an adapted scoring method for human NASH [10]. Briefly, steatosis was determined at a 40-100x magnification and quantified as macrovesicular and microvesicular steatosis, expressed as the percentage of the total surface area. Hepatic inflammation was analyzed by counting the number of inflammatory aggregates in five fields per specimen at a 100x magnification (view size 3.1 mm^2). Inflammatory cell aggregate counts were expressed as the average number of aggregates per field. Early liver fibrosis was evaluated by collagen staining using Picro-Sirius Red (Chroma, WALDECK-Gmbh, Münster, Germany). The level of collagen deposition in the perisinusoidal area was determined relative to the total perisinusoidal area and expressed as a percentage. Correlation between the two forms of steatosis and lobular inflammation were made and validated in independent NASH studies with C57BL/6J mice and LDLr-/-.Leiden mice. More specifically, male C57BL/6J mice (n=12, 12 weeks of age) were treated with the above specified HFD (D12451) for 24 weeks to induce NASH. NAFLD was histologically scored to investigate the potential relationship between micro-/macrovesicular steatosis and lobular inflammation. Male LDLr-/-.Leiden mice (n=12, 12-16 weeks of age) were treated with HFD for 34 weeks to induce a NASH phenotype with liver fibrosis to investigate the association between steatosis and fibrosis. These models can develop NASH after long-term HFD feeding (>20 weeks) with marked lobular inflammation [10,11].

Liver lipid analysis

The intrahepatic concentration of free cholesterol triglycerides, and cholesteryl esters was analyzed as described [7]. Briefly, lipids were extracted from liver homogenates using the Bligh and Dyer method and separated by high performance thin layer chromatography (HPTLC) on silica gel plates. Lipid spots were stained

with color reagent (5g of $MnCl_{24}H_2O$, 32 ml of 95–97% H_2SO_4 added to 960 ml of CH_3OH:H2O 1:1 v/v) and triglycerides, cholesteryl esters and free cholesterol were quantified using TINA version 2.09 software (Raytest, Straubenhardt, Germany).

Biochemical analysis of metabolic parameters

Plasma levels of total cholesterol and triglycerides were measured with commercially available kits (Roche Diagnostics, Almere, The Netherlands). Plasma glucose was determined using the "Freestyle glucose measurement system" (Abbott, Heerlen, The Netherlands). Plasma insulin was quantified by ELISA (Mercodia, Uppsala, Sweden). Serum alanine transaminase (ALT) (GPT, cat. no. 10745138) and aspartate aminotransferase (AST) (GOT, cat. no. 10745120) activities were measured using Reflotron® kits (Roche Diagnostics).

RNA isolation and gene expression analysis

Transcriptome analysis was performed essentially as reported in [12] and references therein. Briefly, total RNA was extracted from individual livers using glass beads and RNAzol (Campro Scientific, Veenendaal, The Netherlands). After quality control of RNA integrity using RNA 6000 Nano Lab-on-a-Chip kit and a bioanalyzer 2100 (Agilent Technologies), biotinylated cRNA was prepared with an Illumina® TotalPrep™ RNA Amplification Kit (Ambion, art.No.AM-IL1791. Biotinylated cRNA was hybridized onto the MouseRef-8 Expression BeadChip (Illumina) by a service provider (Service XS, Leiden, the Netherlands). Genomestudio v1.1.1 software (Illumina) was used for subsequent gene expression analysis. Differentially expressed probes were identified using the limma package of R/Bioconductor. Differentially expressed probes were selected based on the cut-off value False discovery rate (FDR)<0.05. Selected differentially expressed probes were used as an input for pathway analysis using Ingenuity Pathway Analysis suite (http://www.ingenuity.com).

Statistical analysis

Data are presented as mean ± SEM. Significant differences between more than two groups were estimated by one-way ANOVA and Tukey post-hoc analysis

(parametric samples) or Kruskal–Wallis followed by Mann-Whitney U tests (non-parametric samples). Significant differences between two groups were determined by two-sided Student's t-test. Correlations between two variables were calculated by Spearman's rank (non-normally distributed variables) or Pearson's rank (normally distributed variables) correlation coefficient. A p-value<0.05 was considered statistically significant. GraphPad Prism software 6.0 was used for calculations (GraphPad Software, La Jolla, CA).

RESULTS

HFC feeding leads to liver steatosis and lobular inflammation in context of obesity, dyslipidemia and insulin resistance

E3L.CETP mice were treated with HFC up to 12 weeks. Histological analysis of livers showed that HFC-treated mice developed moderate pericentral steatosis after 4 weeks (Figure 1). This early steatosis consisted mainly of microvesicular steatosis. Steatosis intensified until the end of the study (at 12 weeks) and macrovesicular steatosis became more abundant. The development of steatosis can be attributed to a significant increase in liver lipids such as triglycerides (Table 1). With regards to lobular inflammation, first inflammatory cell aggregates were observed after 4 weeks of HFC feeding and more inflammatory aggregates were present at the end of the study (Figure 1).

During the experiment, mice developed an obese phenotype with a significant increase in body weight and visceral (epididymal and mesenteric) white adipose tissue (Table 1). Furthermore, HFC treatment induced dyslipidemia as demonstrated by significant elevations in plasma cholesterol and triglycerides. Mice developed insulin resistance as reflected by increased fasting insulin and glucose concentrations in plasma. Liver enzymes AST and ALT were significantly elevated at the end of the study demonstrating that HFC feeding resulted in hepatocellular damage. In all, HFC feeding resulted in development of NASH in context of diet-induced obesity, dyslipidemia and insulin resistance.

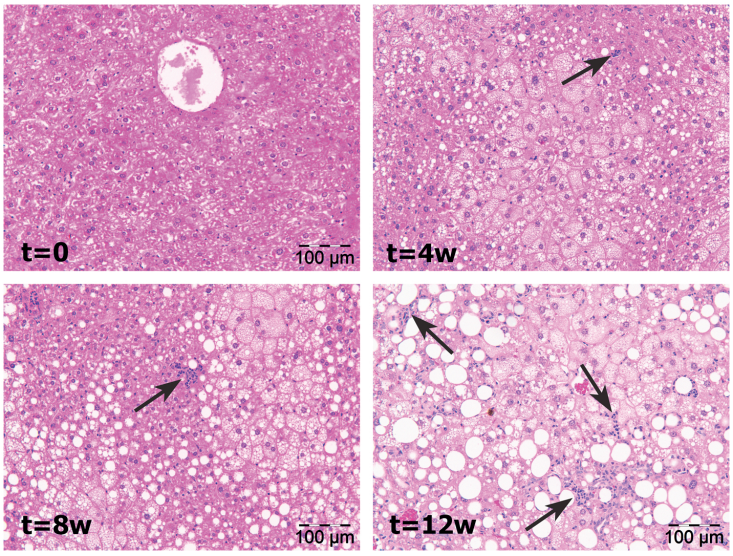

Figure 1. Histological presentation of NASH in E3L.CETP mice. Representative photomicrographs of HE-stained liver cross-sections of E3L.CETP mice fed a high-fat diet supplemented with 1% cholesterol (HFC) for 0, 4, 8 and 12 weeks showing development steatosis and increased lobular inflammation (arrows) over time. (Magnification:x200).

Table 1. Effect of HFC feeding on metabolic parameters over time.

Parameter	t=0	t=4 w	t=8 w	t=12 w
Body weight (g)	29.4 ± 0.6^{a}	36.0 ± 1.0^{b}	42.2 ± 1.6^{c}	47.6 ± 2.0^{d}
Epididymal fat (g)	0.4 ± 0.1^{a}	1.8 ± 0.3^{b}	2.3 ± 0.2^{bc}	2.5 ± 0.2^{c}
Mesenteric fat (g)	0.3 ± 0.0^{a}	0.5 ± 0.1^{a}	0.8 ± 0.1^{b}	0.8 ± 0.1^{b}
Liver (g)	1.8 ± 0.1^{a}	1.8 ± 0.1^{a}	2.4 ± 0.2^{b}	3.1 ± 0.2^{c}
Hepatic lipids (µg/mg protein):				
Triglycerides	83.5 ± 11.9^{a}	171.9 ± 86.6^{b}	321.5 ± 41.8^{c}	304.6 ± 35.8^{c}
Cholesteryl esters	17.9 ± 2.7^{a}	51.3 ± 4.8^{b}	65.8 ± 5.0^{bc}	82.8 ± 6.7^{c}
Free cholesterol	16.9 ± 1.3^{a}	19.2 ± 1.5^{a}	27.6 ± 1.6^{b}	30.5 ± 2.3^{c}
Serum levels, fasting:				
ALT (U/L)	121.7 ± 10.0^{a}	151.2 ± 39.7^{a}	100.8 ± 21.7^{a}	304.8 ± 53.6^{b}
AST (U/L)	270.0 ± 21.3^{a}	341.2 ± 111.6^{ab}	171.9 ± 20.9^{b}	519.6 ± 80.8^{c}
Plasma levels, fasting:				
Glucose (mM)	9.5 ± 0.8^{a}	12.3 ± 0.9^{b}	15.7 ± 0.7^{c}	16.0 ± 0.7^{c}
Insulin (ng/mL)	0.4 ± 0.1^{a}	2.4 ± 0.6^{b}	2.2 ± 0.4^{b}	4.4 ± 0.8^{c}
Cholesterol (mM)	6.7 ± 0.7^{a}	13.3 ± 1.1^{b}	13.7 ± 2.7^{b}	25.9 ± 2.0^{c}
Triglycerides (mM)	3.3 ± 0.5^{a}	2.9 ± 0.3^{a}	2.2 ± 0.6^{a}	6.7 ± 1.1^{b}

Mice were fed a high-fat diet supplemented with 1% (w/w) cholesterol (HFC) diet and groups (n=10) were sacrificed at regular intervals (t=0, t=4, t=8 or t=12 weeks). Values are mean±SEM. ^{a,b,c,d} Mean values within a row with unlike superscript letters are significantly different (p<0.05).

Macrovesicular steatosis is positively associated with development of lobular inflammation

In a more refined histopathological analysis, we quantified the two forms of steatosis as well as the number inflammatory aggregates during HFC feeding. At already 4 weeks of HFC treatment, a pronounced and significant increase in microvesicular steatosis was observed (38%, $p<0.05$; Figure 2A). After this rapid induction, microvesicular steatosis remained at a constant elevated level until the end of the study. By contrast, macrovesicular steatosis showed a gradual and continuous development over time (24% at week 12, $p<0.05$; Figure 2B). The number of inflammatory cell aggregates increased significantly after 4 weeks and showed a further increase at 12 weeks of HFC treatment (Figure 2C). Next, we examined whether a potential relationship exists between micro-/macrovesicular steatosis and lobular inflammation. Correlation analysis revealed a positive association between macrovesicular steatosis and inflammatory cell aggregates ($r=0.45$; $p=0.01$; Figure 2D). By contrast, microvesicular steatosis and total hepatic triglyceride content were not correlated with inflammatory cell aggregates ($r=0.05$; $p=0.8$ and $r=-0.05$; $p=0.8$, respectively). Together, these results indicate that a specific type of steatosis, macrovesicular steatosis, is critical for the development of lobular inflammation in NASH.

Macrovesicular steatosis and inflammatory cell aggregates are associated independent of the disease model

The positive association between macrovesicular steatosis and lobular inflammation observed in E3L.CETP mice was examined in other models of obesity-induced NASH. More specifically, we examined livers of a mild experimental model (HFD-treated C57BL/6J mice) and a more severe model (HFD-treated LDLr-/-.Leiden mice). C57BL/6J mice developed steatosis (macrovesicular: 23.3±2.2%; microvesicular: 59.5±2.0% of total surface area) with modest inflammation (inflammatory aggregates: 2.0±0.5 per microscopic field) (Figure 3A). LDLr-/-.Leiden mice also developed steatosis (macrovesicular: 26.5±2.3%; and microvesicular: 30.5±2.5% of total surface area), but more inflammatory aggregates (45.9±12.6 per microscopic field) and marked fibrosis (23.4±5.1%) (Figure 3A). To examine the relationship between macrovesicular steatosis and inflammation, we compared mice with a high

and low level of macrovesicular steatosis, and comparable microvesicular steatosis. In both NASH models, macrovesicular steatosis above 20% was associated with significant increases in inflammatory aggregates (Figure 3B-C). Again, macrovesicular steatosis was positively correlated with inflammatory aggregates (C57BL/6J: r=0.66, and LDLr-/-.Leiden: r=0.77; both p<0.05), while no correlation was observed for microvesicular steatosis (not shown).

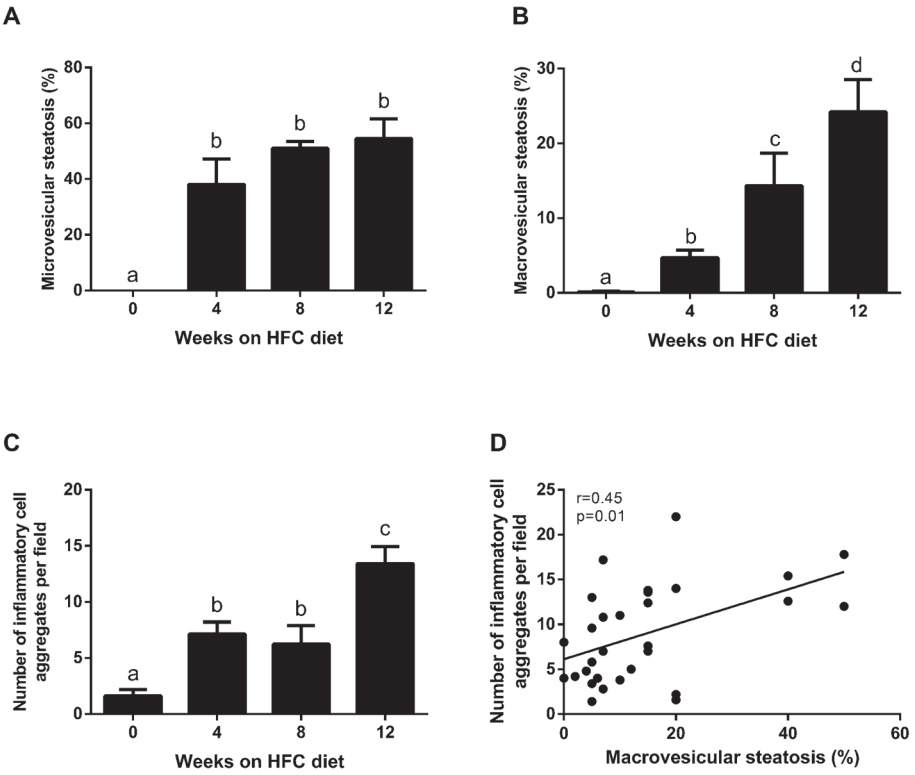

Figure 2. Quantitative histological analysis of the development of liver steatosis and inflammation in E3L.CETP mice. Quantification of the two steatosis forms (A) microvesicular steatosis and (B) macrovesicular steatosis expressed as percentage (%) of the total surface area. Microvesicular steatosis developed rapidly after 4 weeks of HFC and levels remained constant over time, whereas macrovesicular steatosis developed continuously. (C) Lobular inflammation (expressed as the number of inflammatory cell aggregates per field) was induced already after 4 weeks of HFC but increased strongly after 12 weeks of HFC feeding. (D) Macrovesicular steatosis is positively correlated with inflammatory cell aggregates as determined by Spearman's rank correlation analysis. [a,b,c,d] Mean values with unlike letters differ significantly from each other ($p \leq 0.05$).

Macrovesicular steatosis is associated with the development of fibrosis

Next, we investigated whether there is a link between the development of macrovesicular steatosis and liver fibrosis. Sirius red staining of livers from the time course experiment in E3L.CETP mice showed mild perihepatocellular fibrosis at end point (12 weeks of HFC treatment) (Figure 4A). Specifically for the 12-week time point, we observed a significant upregulation of genes involved in pro-fibrotic pathways including TGFβ, TIMP-1, Col1α1, Col1α2 and MMP13 (Figure 4B) as demonstrated by microarray pathway analysis. Of note, this onset of fibrosis was observed when macrovesicular steatosis reached levels above 20%.

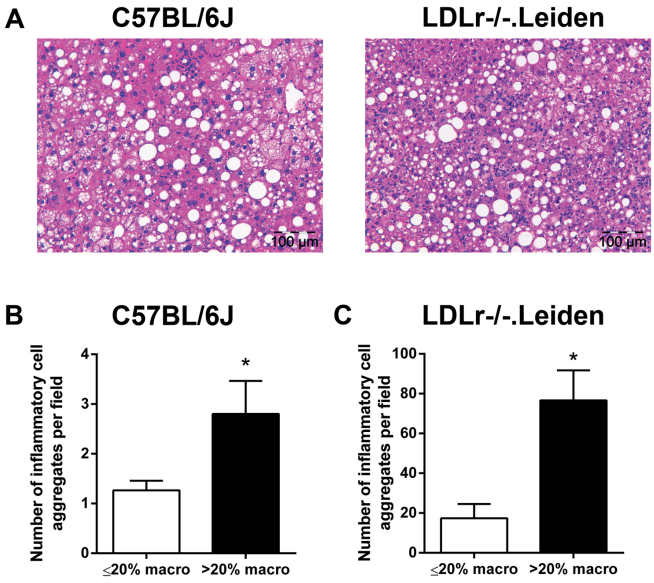

Figure 3. Histological representation and the role of macrovesicular steatosis in other diet-induced NASH mouse models. Representative photographs of HE-stained liver cross-sections from (A) male C57BL/6J mice fed a high-fat diet (HFD) for 24 weeks and male LDLr-/-.Leiden mice treated with HFD for 34 weeks. Photomicrographs on the left show C57BL/6J and on the right LDLr-/-.Leiden mice (Magnification: x200). (B) C57BL/6J mice with high levels of macrovesicular steatosis (>20%) showed more inflammatory cell aggregates then mice with low levels of macrovesicular steatosis (≤ 20%), while microvesicular steatosis was comparable (high vs. low macrovesicular steatosis: ±53% vs. ±60%, respectively). (C) LDLr-/- mice with high levels of macrovesicular (>20%) have increased lobular inflammation compared to mice with low macrovesicular steatosis (≤20%), while microvesicular steatosis was comparable between the groups (both, ±30%).

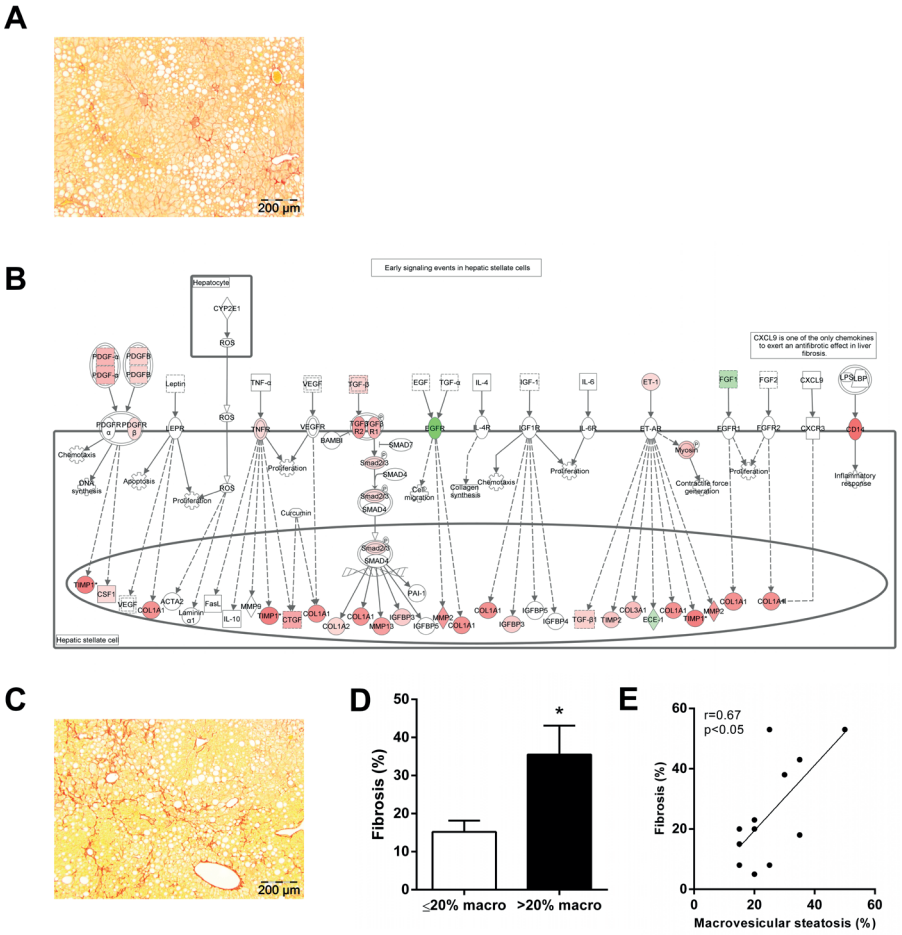

Figure 4. Onset of liver fibrosis in E3L.CETP mice and established fibrosis in LDLr-/-.Leiden mice. (A) Representative photomicrograph of pico-sirius red-stained livers from E3L.CETP mice showing mild fibrosis (Magnification x100). Arrows show perihepatocellular fibrosis. (B) Transcriptome analysis confirmed the onset of liver fibrosis as demonstrated by upregulation of pro-fibrotic signaling pathways in hepatic stellate cells and showed increased expression of pro-fibrotic genes including *Col-1α, Timp1, Smad3*. Nodes that are colored red (upregulated) or green (downregulated) indicate significant differences in fold-change in HFC-fed mice compared to HFD-fed control mice. (C) Representative photomicrograph of pico-sirius red-stained liver section showing pronounced fibrosis in LDLr-/-.Leiden mice treated with HFD feeding for 34 weeks (Magnification x100). (D) LDLr-/-.Leiden mice with high levels of macrovesicular (>20%) have more fibrosis compared to mice with low macrovesicular steatosis (≤20%). (E) Macrovesicular steatosis is positively correlated with fibrosis in HFD-fed LDLr-/-.Leiden mice.

The relationship between macrovesicular steatosis and liver fibrosis was further examined in a NASH model with pronounced fibrosis, namely LDLr-/-.Leiden mice (Figure 4C). LDLr-/-.Leiden mice with a high percentage of macrovesicular steatosis (>20%) exhibited more fibrosis than mice with a low level of macrovesicular steatosis (≤20%) (Figure 4D). Furthermore, the level of macrovesicular steatosis correlated positively with the amount of liver fibrosis ($r=0.67$, $p<0.05$, Figure 4E) while there was no correlation between microvesicular steatosis and fibrosis. Of note, the number of inflammatory cell aggregates is strongly correlated with fibrosis ($r=0.93$, $p<0.001$). Thus, the association between macrovesicular steatosis and fibrosis is likely to be a consequence of the development of macrovesicular steatosis-associated lobular inflammation. Altogether, these results support the importance of macrovesicular steatosis in the etiology of liver inflammation and, as a consequence thereof, liver fibrosis.

DISCUSSION

This study analyzed the progression of steatosis and inflammation during the pathogenesis of NASH in obesity. Specifically, we examined the relationship between the development of specific forms of steatosis and inflammatory cell aggregates in different diet-induced NASH models. In E3L.CETP mice treated with a high-fat diet containing 1% w/w cholesterol (HFC), a rapid induction of microvesicular steatosis was observed (at week 4). This form of steatosis remained at an elevated level and did not further progress. By contrast, macrovesicular steatosis showed a progressive development until the end of the study (week 12). Development of macrovesicular steatosis correlated positively with the number of inflammatory cell aggregates, whereas microvesicular steatosis did not correlate with inflammation. Further support for a positive association between macrovesicular steatosis and lobular inflammation was obtained from independent NASH studies in HFD-treated C57BL/6J and LDLr-/-.Leiden. Furthermore, macrovesicular steatosis was positively associated with perihepatocellular fibrosis in LDLr-/-.Leiden mice, a mouse model that develops

pronounced liver fibrosis on a HFD. Collectively, these results highlight the importance of macrovesicular steatosis in the pathogenesis of NASH.

In the present study, the diet-induced NASH models showed pronounced development of microvesicular and macrovesicular steatosis. Our time course analysis in E3L.CETP mice revealed that the development of microvesicular steatosis is rapid process and plateau levels were reached after 4 weeks of HFC feeding. By contrast, macrovesicular steatosis developed continuously and progressively over time. The development of these two forms of steatosis is only poorly understood. It is not clear whether the small lipid vacuoles (microvesicular steatosis) fuse to form one large vacuole (macrovesicular steatosis), or whether macrovesicular and microvesicular steatosis develop independently from each other ([13] and references therein). The most widely accepted theory of lipid droplet biogenesis implies that neutral glycerol and esters accumulate within the phospholipid bilayer of the endoplasmatic reticulum (ER) and the bilayer gradually separates from the ER to form nascent phospholipid-coated lipid droplets which bud off into the cytosol [13-15]. The most common form of further growth of these droplets is expansion by diffusion of lipids (from the ER or cytosol), i.e. triglycerides are added to the cores and phospholipids as surfactants to the surfaces of a growing lipid droplet. Notably, the fusion of small lipid vacuoles to a large vacuole is considered to be a relatively rare event [13,14]. Thus, it is possible that the observed gradual development of macrovesicular steatosis may be determined by the amount of phospholipids that are available in a hepatocyte to enlarge the microvesicular structures.

The large lipid droplets that are characteristic for macrovesicular steatosis can cause cellular stress and architectural changes to hepatocytes [13]. The injured liver cells then release immune reactive substances and hepatocellular damage will ultimately lead to ballooning, apoptosis and infiltration of immune cells [16]. Consistent with these processes, we observed a significant correlation between macrovesicular steatosis and immune cell aggregates in all models. Absence of a correlation between inflammatory cell aggregates and microvesicular steatosis suggests that the microvesicular lipid droplets are less harmful. The importance of macrovesicular steatosis as inducer of liver injury and subsequent liver fibrosis is supported by a recent study in rats [17]. A comparison of different rat strains

with either 1) solely microvesicular steatosis (Lewis rats), 2) pure macrovesicular steatosis (Sprague Dawley) and 3) mixed-type steatosis (Wistar) showed that Sprague Dawley rats with macrovesicular steatosis had the highest degree of lobular inflammation and fibrosis [17]. In line with this, we observed that the marked increase in macrovesicular steatosis between 8 and 12 weeks of HFC feeding in E3L.CETP mice is accompanied by increased number of inflammatory cell aggregates, and onset of pathways leading to liver fibrosis. Furthermore, macrovesicular steatosis and inflammatory cell aggregates correlated significantly with the level of hepatocellular fibrosis in the LDLr-/-.Leiden mice.

This study used different mouse strains and diets to investigate the development of NASH in the context of visceral obesity, insulin resistance and dyslipidemia, all of which constitute important risk factors of NAFLD in humans [1-3]. These risk factors are not or only inadequately mimicked in methionine choline deficient (MCD) diet-induced NAFLD or CCl4-induced liver fibrosis [18,19]. It is generally assumed that diets low in methionine and choline are required to induce liver fibrosis [18]. However, the present study shows that liver fibrosis can also be induced with high-fat diets (HFD) containing 45 energy percent from fat, which is translational to human diets [20]. We have previously reported that LDLr-/-.Leiden mice develop a NASH phenotype on HFD which reflects human steatohepatitis [10]. We herein show that these animals develop pronounced liver fibrosis (>20% perihepatocellular fibrosis) when the HFD treatment is prolonged (34 weeks). Consistent with this observation, others reported that mice on a LDLr-/- background constitute a physiological model particularly vulnerable to study the inflammation in NAFLD [21].

High-fat diets are often supplemented with cholesterol to induce chronic liver inflammation. In LDLr-/- mice, Bieghs and coworkers demonstrated that cholesterol feeding can cause lysosomal cholesterol accumulation in Kupffer cells which correlates with hepatic inflammation and cholesterol crystallization [22]. Similarly, E3L mice treated with a Western-type diet containing 1% (w/w) cholesterol for 20 weeks show formation of cholesterol crystals and collagen deposition in liver [23] as they have been described in humans with NASH [24]. Consistent with this pro-fibrotic effect of dietary cholesterol, HFC-fed E3L.CETP mice developed early fibrosis after already 12 weeks, and transcriptome analysis substantiated the

activation of pro-fibrotic signaling pathways in liver controlled by TNF, PDGF and TGFβ. The same pathways were activated in mouse liver with high (1% w/w) but not low (0.25% w/w) dietary cholesterol [25]. This effect was attributable to dietary cholesterol itself and not to the fat content of the diet. Therefore, it is likely that NASH-inducing diets containing high concentrations of cholesterol accentuate the above mentioned inflammatory pathways, and that other inflammatory pathways which also may contribute to NASH development (e.g. IL-6 and leptin signaling) have a relative lower contribution.

In all, our data highlight the importance of macrovesicular steatosis in the pathogenesis of experimental diet-induced NASH, because this form steatosis is tightly associated with cellular lobular inflammation and perihepatocellular fibrosis. Our study advocates a more refined morphological analysis of steatosis subtypes in addition to biochemical liver lipid analysis. Such an analysis may be of particular relevance for efficacy studies with nutritional or pharmaceutical interventions.

ACKNOWLEDGEMENTS

The authors gratefully acknowledge Erik Offerman and Wim van Duyvenvoorde for technical assistance. This study was supported by the TNO research programs ‘Personalized Prevention and Therapy/Predictive Health Technologies PHT’ (to Petra Mulder). The research was performed within the framework of CTMM, the Center for Translational Molecular Medicine (www.ctmm.nl), project PREDICCT (to Wen Liang).

REFERENCES

1. Vernon G, Baranova A, Younossi ZM. Systematic review: the epidemiology and natural history of non-alcoholic fatty liver disease and non-alcoholic steatohepatitis in adults. Alimentary pharmacology & therapeutics 2011;34:274-285.
2. Loomba R, Sanyal AJ. The global NAFLD epidemic. Nature reviews Gastroenterology & hepatology 2013;10:686-690.
3. Bellentani S, Marino M. Epidemiology and natural history of non-alcoholic fatty liver disease (NAFLD). Annals of hepatology 2009;8 Suppl 1:S4-8.
4. Green CJ, Hodson L. The influence of dietary fat on liver fat accumulation. Nutrients 2014;6:5018-5033.
5. Neuschwander-Tetri BA. Hepatic lipotoxicity and the pathogenesis of nonalcoholic steatohepatitis: the central role of nontriglyceride fatty acid metabolites. Hepatology 2010;52:774-788.
6. Farrell GC, van Rooyen D, Gan L, Chitturi S. NASH is an Inflammatory Disorder: Pathogenic, Prognostic and Therapeutic Implications. Gut and liver 2012;6:149-171.
7. Liang W, Lindeman JH, Menke AL, Koonen DP, Morrison M, Havekes LM, et al. Metabolically induced liver inflammation leads to NASH and differs from LPS- or IL-1beta-induced chronic inflammation. Laboratory investigation; a journal of technical methods and pathology 2014;94:491-502.
8. Ueha S, Shand FH, Matsushima K. Cellular and molecular mechanisms of chronic inflammation-associated organ fibrosis. Frontiers in immunology 2012;3:71.
9. Liang W, Tonini G, Mulder P, Kelder T, van Erk M, van den Hoek AM, et al. Coordinated and interactive expression of genes of lipid metabolism and inflammation in adipose tissue and liver during metabolic overload. PloS one 2013;8:e75290.
10. Liang W, Menke AL, Driessen A, Koek GH, Lindeman JH, Stoop R, et al. Establishment of a general NAFLD scoring system for rodent models and comparison to human liver pathology. PloS one 2014;9:e115922.
11. Ito M, Suzuki J, Tsujioka S, Sasaki M, Gomori A, Shirakura T, et al. Longitudinal analysis of murine steatohepatitis model induced by chronic exposure to high-fat diet. Hepatology research : the official journal of the Japan Society of Hepatology 2007;37:50-57.
12. Verschuren L, Wielinga PY, Kelder T, Radonjic M, Salic K, Kleemann R, et al. A systems biology approach to understand the pathophysiological mechanisms of cardiac pathological hypertrophy associated with rosiglitazone. BMC medical genomics 2014;7:35-8794-8797-8735.
13. Sahini N, Borlak J. Recent insights into the molecular pathophysiology of lipid droplet formation in hepatocytes. Progress in lipid research 2014;54:86-112.
14. Wilfling F, Wang H, Haas JT, Krahmer N, Gould TJ, Uchida A, et al. Triacylglycerol synthesis enzymes mediate lipid droplet growth by relocalizing from the ER to lipid droplets. Dev Cell 2013;24:384-399.
15. Guo Y, Cordes KR, Farese RV, Jr., Walther TC. Lipid droplets at a glance. J Cell Sci 2009;122:749-752.
16. Baffy G. Kupffer cells in non-alcoholic fatty liver disease: the emerging view. Journal of hepatology 2009;51:212-223.
17. Rosenstengel S, Stoeppeler S, Bahde R, Spiegel HU, Palmes D. Type of steatosis influences microcirculation and fibrogenesis in different rat strains. Journal of investigative surgery : the official journal of the Academy of Surgical Research 2011;24:273-282.

18. Rosso N, Chavez-Tapia NC, Tiribelli C, Bellentani S. Translational approaches: from fatty liver to non-alcoholic steatohepatitis. World journal of gastroenterology : WJG 2014;20:9038-9049.
19. Rinella ME, Green RM. The methionine-choline deficient dietary model of steatohepatitis does not exhibit insulin resistance. Journal of hepatology 2004;40:47-51.
20. Hu FB, Manson JE, Willett WC. Types of dietary fat and risk of coronary heart disease: a critical review. Journal of the American College of Nutrition 2001;20:5-19.
21. Bieghs V, Van Gorp PJ, Wouters K, Hendrikx T, Gijbels MJ, van Bilsen M, et al. LDL receptor knock-out mice are a physiological model particularly vulnerable to study the onset of inflammation in non-alcoholic fatty liver disease. PloS one 2012;7:e30668.
22. Bieghs V, Walenbergh SM, Hendrikx T, van Gorp PJ, Verheyen F, Olde Damink SW, et al. Trapping of oxidized LDL in lysosomes of Kupffer cells is a trigger for hepatic inflammation. Liver international : official journal of the International Association for the Study of the Liver 2013;33:1056-1061.
23. Morrison MC, Liang W, Mulder P, Verschuren L, Pieterman E, Toet K, et al. Mirtoselect, an anthocyanin-rich bilberry extract, attenuates non-alcoholic steatohepatitis and associated fibrosis in ApoE(*)3Leiden mice. Journal of hepatology 2015;62:1180-1186.
24. Ioannou GN, Haigh WG, Thorning D, Savard C. Hepatic cholesterol crystals and crown-like structures distinguish NASH from simple steatosis. Journal of lipid research 2013;54:1326-1334.
25. Kleemann R, Verschuren L, van Erk MJ, Nikolsky Y, Cnubben NH, Verheij ER, et al. Atherosclerosis and liver inflammation induced by increased dietary cholesterol intake: a combined transcriptomics and metabolomics analysis. Genome biology 2007;8:R200.